A second-order Markov process for modeling diffusive motion through spatial discretization

Marco Sant, George K. Papadopoulos, and Doros N. Theodorou

Citation: J. Chem. Phys. **128**, 024504 (2008); doi: 10.1063/1.2813416
View online: http://dx.doi.org/10.1063/1.2813416
View Table of Contents: http://jcp.aip.org/resource/1/JCPSA6/v128/i2
Published by the American Institute of Physics.

A second-order Markov process for modeling diffusive motion through spatial discretization

Marco Sant, George K. Papadopoulos, and Doros N. Theodorou[a)]
School of Chemical Engineering, National Technical University of Athens, 9 Heroon Polytechniou Street, Zografou Campus, Athens 15780, Greece

(Received 25 September 2007; accepted 25 October 2007; published online 11 January 2008)

A new "mesoscopic" stochastic model has been developed to describe the diffusive behavior of a system of particles at equilibrium. The model is based on discretizing space into slabs by drawing equispaced parallel planes along a coordinate direction. A central role is played by the probability that a particle exits a slab via the face opposite to the one through which it entered (transmission probability), as opposed to exiting via the same face through which it entered (reflection probability). A simple second-order Markov process invoking this probability is developed, leading to an expression for the self-diffusivity, applicable for large slab widths, consistent with a continuous formulation of diffusional motion. This model is validated via molecular dynamics simulations in a bulk system of soft spheres across a wide range of densities. © *2008 American Institute of Physics*. [DOI: 10.1063/1.2813416]

I. INTRODUCTION

To calculate the self-diffusivity D_s of a fluid system comprising N particles under equilibrium, subject to thermal motion, an average of the mean square $\langle \mathbf{r}^2(t) \rangle = (1/N)\Sigma_{i=1}^{N} \mathbf{r}_i^2(t)$ of the displacement vectors $\mathbf{r}_i$ of all particles or, equivalently, an orientational average of the mean squares of the displacements x_i, y_i, and z_i of all particles along each spatial coordinate is performed over the elapsed time t, according to the Einstein relation[1]

$$D_s = \lim_{t\to\infty} \frac{d}{dt} \frac{\langle \mathbf{r}^2(t) \rangle}{2d_0} = \frac{1}{d_0} \left\{ \lim_{t\to\infty} \frac{d}{dt} \frac{\langle x^2(t) \rangle}{2} + \lim_{t\to\infty} \frac{d}{dt} \frac{\langle y^2(t) \rangle}{2} + \lim_{t\to\infty} \frac{d}{dt} \frac{\langle z^2(t) \rangle}{2} \right\}, \tag{1}$$

where $d_0 = 3$ is the dimensionality of the system under consideration.

Through Eq. (1), an independent calculation of the self-diffusivity component along each direction is enabled, leading to a simpler approach to the problem. In the present work, diffusion was studied along only one direction, for computational convenience.

The aim of this paper is to develop a "mesoscopic" model for the system dynamics, capable to coarse grain the motion of the particles, while preserving the system self-diffusivity. In contrast to most models, the new model will be based on a spatial, as opposed to temporal, discretization of the system. This has certain advantages in understanding the dependence of diffusivity on density and on the possible presence of external force fields, for example, within a microporous medium. The new model will allow the representation of the coefficient of self-diffusivity as the product of two functions, one having to do with the unidirectional molecular flux through a test surface at any instant and the other with the tendency of molecules to reverse their direction of motion due to collisions with other molecules.

II. MODEL DEVELOPMENT

A. Definitions

Without loss of generality, we study the dynamics of a bulk system consisting of spherical particles interacting through a soft repulsive potential (see Sec. III B), at temperature T, with periodic boundary conditions in all three directions. The simulation box of the system to be modeled is divided into consecutive slabs by a series of equispaced parallel planes, normal to the x direction, placed at a distance l from each other. The simulation box length in the x direction is an integer multiple of l. The volume of the simulation box is V and the total number of particles in it is N (see Fig. 1).

We consider a particle entering a slab in the course of thermal motion at equilibrium. Having entered, the particle will eventually exit the slab for the first time in one of two ways: it will either wander through the whole slab and exit via the face opposite to the one through which it entered, its direction of motion along x at the point of exit being the same as when it originally entered the slab (transmission event), or it will spend some time in the slab and exit via the same face through which it entered, its direction of motion at the point of exit being opposite to the direction of its entry (reflection event). We denote by P the conditional probability that the particle exits the slab through a transmission event. Then, $(1-P)$ will be the conditional probability that the particle exits the slab through a reflection event. We will call P the transmission probability. A mean residence time τ is defined as the average time spent by a particle inside a slab between its entry to and first exit from the slab.

a)Author to whom correspondence should be addressed. Electronic mail: doros@central.ntua.gr.

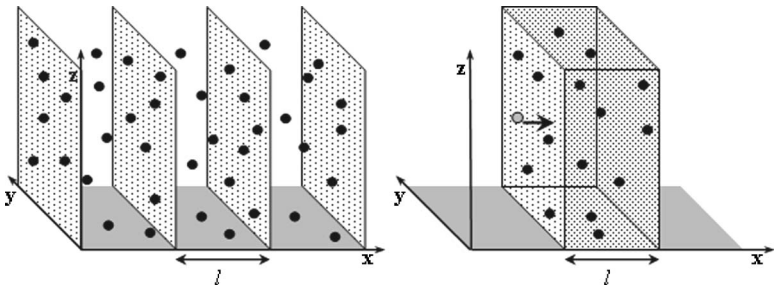

FIG. 1. Space discretization of the system through parallel planes (left) and detail of a particle entering an individual slab (right).

B. Theoretical concepts

At this point, the motion of a particle along the x direction can be represented, in a coarse-grained fashion, through a stochastic chain of events subject to certain rules for crossing the imaginary surfaces, or "checkpoints," which form the boundaries between successive slabs.

The process, illustrated in Fig. 2, is a second-order Markov chain. The states adopted by the particle are denoted as $i+$ and $i-$, with i being the index of the dividing surface (checkpoint) traversed by the particle. State $i+$ corresponds to the particle traversing dividing surface i in the positive x direction (moving from left to right, component of particle velocity $v_x>0$). State $i-$ corresponds to the particle traversing dividing surface i in the negative x direction (moving from right to left, component of particle velocity $v_x<0$). From state $i+$, a transition may occur either to state $(i+1)+$ (transmission event with particle exiting the slab, delimited by dividing surfaces i and $i+1$, through dividing surface $i+1$) or to state $i-$ (reflection event with particle exiting the slab, delimited by dividing surfaces i and $i+1$, through dividing surface i). The transition probabilities are P and $(1-P)$, respectively, with P being the transmission probability, as defined above. Similarly, from state $i-$, a transition may occur either to state $(i-1)-$ (transmission event with particle exiting the slab, delimited by dividing surfaces $i-1$ and i, through dividing surface $i-1$) or to state $i+$ (reflection event with particle exiting the slab, delimited by dividing surfaces $i-1$ and i, through dividing surface i). Again, the transition probabilities are P and $(1-P)$, respectively. Denoting by $\Pi^+(i,k)$ $[\Pi^-(i,k)]$, the *a priori* probability of being in state $i+$ $(i-)$ after the kth transition in the system, we can write the coupled master equations,

$$\Pi^+(i,k) = \Pi^+(i-1,k-1)P + \Pi^-(i,k-1)(1-P), \tag{2a}$$

$$\Pi^-(i,k) = \Pi^-(i+1,k-1)P + \Pi^+(i,k-1)(1-P). \tag{2b}$$

Denoting by x_k and $v_{x,k}$ the x components of the position and velocity vectors of a particle after k transitions, respectively, the following relations hold:

$$\left.\begin{aligned} x_{k+1} &= x_k + \frac{v_{x,k}}{|v_{x,k}|}l \\ \frac{v_{x,k+1}}{|v_{x,k+1}|} &= \frac{v_{x,k}}{|v_{x,k}|} \end{aligned}\right\} \text{ with probability } P,$$

and

$$\left.\begin{aligned} x_{k+1} &= x_k \\ \frac{v_{x,k+1}}{|v_{x,k+1}|} &= -\frac{v_{x,k}}{|v_{x,k}|} \end{aligned}\right\} \text{ with probability } 1-P.$$

By definition of the mean residence time in a slab τ, the total elapsed time t is related to the number of transitions k through

$$t = k\tau \quad (k \gg 1). \tag{3}$$

On the other hand, the continuous spatial variable x is related to the index i through

$$x = il. \tag{4}$$

Note that $k=0$ corresponds to the time origin $t=0$.

As an initial condition, we may consider that the particle is traversing the checkpoint $x=0$, moving to the right,

$$\Pi^+(0,0) = 1, \quad \Pi^+(i,0) = 0 \ \forall \ i \neq 0 \text{ and } \Pi^-(i,0) = 0 \ \forall \ i.$$

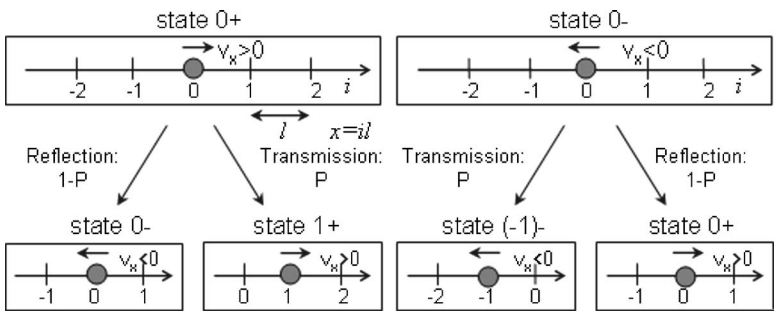

FIG. 2. Representation of the second-order Markov process for the particle position and direction of motion.

Π^- can readily be eliminated from the pair of master equations (2) to obtain a single equation in Π^+. Considering Eq. (2a) with $i+1$ in place of i, one obtains

$$\Pi^+(i+1,k) - \Pi^+(i,k-1) = [\Pi^-(i+1,k-1) - \Pi^+(i,k-1)](1-P).$$

On the other hand, from Eq. (2b),

$$\Pi^-(i+1,k-1) - \Pi^-(i,k) = [\Pi^-(i+1,k-1) - \Pi^+(i,k-1)](1-P).$$

Combining the last two equations,

$$\Pi^+(i+1,k) - \Pi^+(i,k-1) = \Pi^-(i+1,k-1) - \Pi^-(i,k). \tag{5}$$

Equation (2a) with $i+1$ in place of i reads

$$\Pi^+(i+1,k) = \Pi^+(i,k-1)P + \Pi^-(i+1,k-1)(1-P),$$

while Eq. (2a) with $k+1$ in place of k reads

$$\Pi^+(i,k+1) = \Pi^+(i-1,k)P + \Pi^-(i,k)(1-P).$$

Subtracting the last two equations from each other,

$$\Pi^+(i+1,k) - \Pi^+(i,k+1) = \Pi^+(i,k-1)P - \Pi^+(i-1,k)P + [\Pi^-(i+1,k-1) - \Pi^-(i,k)] \times (1-P),$$

and substituting the term in brackets from Eq. (5),

$$\Pi^+(i+1,k) - \Pi^+(i,k+1) = \Pi^+(i,k-1)P - \Pi^+(i-1,k)P + [\Pi^+(i+1,k) - \Pi^+(i,k-1)] \times (1-P),$$

which, upon rearrangement, leads to

$$\Pi^+(i,k+1) = \Pi^+(i-1,k)P + \Pi^+(i+1,k)P + \Pi^+(i,k-1) \times (1-2P). \tag{6}$$

Equation (6) makes evident the second-order Markov character of the considered process. It can be rewritten as

$$[\Pi^+(i,k+1) - \Pi^+(i,k)] + (1-2P)[\Pi^+(i,k) - \Pi^+(i,k-1)] = P[\Pi^+(i-1,k) + \Pi^+(i+1,k) - 2\Pi^+(i,k)]. \tag{7}$$

The quantities within brackets in Eq. (7) can be considered as finite difference estimates of the temporal and spatial derivatives of a continuous function $\Pi^+(x,t)$. Taking into account Eqs. (3) and (4), we can write, for time scales $t \gg \tau$ and length scales $|x| \gg l$,

$$\tau \frac{\partial \Pi^+}{\partial t} + (1-2P)\tau \frac{\partial \Pi^+}{\partial t} = Pl^2 \frac{\partial^2 \Pi^+}{\partial x^2}$$

or

$$\frac{\partial \Pi^+}{\partial t} = \frac{1}{2}\frac{l^2}{\tau}\frac{P}{1-P}\frac{\partial^2 \Pi^+}{\partial x^2}. \tag{8}$$

The above relation is a one-dimensional diffusion equation with the self-diffusion coefficient D_s given by

$$D_s = \frac{1}{2}\frac{l^2}{\tau}\frac{P}{1-P}. \tag{9}$$

One can readily show that Eq. (8) is obeyed by Π^- as well. We have shown that our mesoscopic second-order Markov process model [Eq. (2)] reduces to a diffusion equation when motion over long times (in comparison with the residence time in a slab) and long displacements (in comparison with the slab width) is considered and that the self-diffusivity is simply related to the parameters of the mesoscopic model.

C. Derivation of Equation (9) for a continuous diffusive system

One can try to approach Eq. (9) "top down" from the macroscopic side. Envision a macroscopic system wherein particle motion is described by the continuous one-dimensional diffusion equation,

$$D_s \frac{\partial^2 c}{\partial x^2} = \frac{\partial c}{\partial t}, \tag{10}$$

with $c(x,t)$ being the concentration of labeled particles at position x at time t. We consider the system being partitioned into slabs of width l, which is large in comparison with the distance of velocity randomization, so that motion within each slab is satisfactorily described by the continuous diffusion equation [Eq.(10)] (compare Fig. 1). Focusing our attention on a single slab, $0<x<l$, we ask the question, what is the probability P that a particle which entered the slab will exit it for the first time via the opposite face to the one through which it entered. Hopefully, the solution to this continuum problem will lead to a relation equivalent to Eq. (9).

As initial condition, we want to impose that the labeled particles all enter through a face $x=0$ at time $t=0$, moving from left to right. Since the distribution of velocities is not accounted for in our spatial diffusion equation, we must somehow impose the condition of moving from left to right through the initial position distribution of labeled particles. Here, we impose the initial condition

$$c(x,0) = \frac{N}{V} l \delta(\lambda) \quad (0 < \lambda \ll l), \tag{11}$$

where, as above, N/V is the mean density of (labeled) particles in the system and $\delta(\lambda)$ is a Dirac delta function. The idea is that, at time $t=0+$, all labeled particles find themselves a short distance λ to the right of the origin, having traversed the origin in the direction from left to right. The length λ should be commensurate with the distance traveled by a particle before its direction of motion is randomized through collisions. It can be estimated from the self-diffusivity and the mean molecular speed along the x direction through[2]

$$D_s = \frac{1}{2}\langle |v_x| \rangle \lambda \quad \text{or} \quad \lambda = \frac{2D_s}{\langle |v_x| \rangle}. \tag{12}$$

As posed above, the problem of calculating P is a first-passage problem. To follow the concentration of those particles which have not exited the slab, we must impose absorbing boundary conditions at $x=0$ and $x=l$,

$$c(0,t) = c(l,t) = 0. \tag{13}$$

The solution of Eq. (10) subject to the initial condition [Eq. (11)] and the boundary conditions [Eq.(13)] is readily obtained in series form by separation of variables,[3]

$$c(x,t) = 2\frac{N}{V}\sum_{n=1}^{\infty} \sin\left(\frac{n\pi\lambda}{l}\right)\sin\left(\frac{n\pi x}{l}\right)e^{-(n^2\pi^2/l^2)D_s t}. \tag{14}$$

The magnitude of the flux of labeled particles (particles per unit cross-sectional area per unit time) exiting the slab at $x=l$ at any time t is obtained as

$$|J(t)|_{x=l} = J(t)|_{x=l} = -D_s\left.\frac{\partial c}{\partial x}\right|_{x=l} = \frac{N}{V}\frac{2\pi D_s}{l}\sum_{n=1}^{\infty} n(-1)^{n+1} \times \sin\left(\frac{n\pi\lambda}{l}\right)e^{-(n^2\pi^2/l^2)D_s t}. \tag{15}$$

Similarly, the magnitude of the flux of labeled particles existing the slab at $x=0$ at any time t is

$$|J(t)|_{x=0} = -J(t)|_{x=0} = D_s\left.\frac{\partial c}{\partial x}\right|_{x=0} = \frac{N}{V}\frac{2\pi D_s}{l}\sum_{n=1}^{\infty} n \times \sin\left(\frac{n\pi\lambda}{l}\right)e^{-(n^2\pi^2/l^2)D_s t}. \tag{16}$$

Comparing Eqs. (14)–(16), it is straightforward to show that the following simple mass balance is satisfied at any time t:

$$|J(t)|_{x=0} + |J(t)|_{x=l} = -\frac{d}{dt}\int_0^l c(x,t)dx.$$

The total number of labeled particles that will exit through $x=l$ at all times will be

$$A\int_0^{\infty} |J(t)|_{x=l}dt = A\frac{N}{V}\frac{2l}{\pi}\sum_{n=1}^{\infty}\frac{(-1)^{n+1}}{n}\sin\left(\frac{n\pi\lambda}{l}\right),$$

where A stands for the slab cross-sectional area. By Eq. (11), the total number of particles initially in the slab is $A\int_0^l c(x,0)dx = (N/V)(Al)$. Hence, the fraction of particles that exit through $x=l$ (in the "transmission" direction) is

$$P = \frac{A\int_0^{\infty}|J(t)|_{x=l}dt}{\frac{N}{V}(Al)} = \frac{2}{\pi}\sum_{n=1}^{\infty}\frac{(-1)^{n+1}}{n}\sin\left(\frac{n\pi\lambda}{l}\right). \tag{17}$$

On the other hand, from Eqs. (15) and (16),

$$\frac{P}{1-P} = \frac{\int_0^{\infty}|J(t)|_{x=l}dt}{\int_0^{\infty}|J(t)|_{x=0}dt} = \frac{\frac{2}{\pi}\sum_{n=1}^{\infty}\frac{(-1)^{n+1}}{n}\sin\left(\frac{n\pi\lambda}{l}\right)}{\frac{2}{\pi}\sum_{n=1}^{\infty}\frac{1}{n}\sin\left(\frac{n\pi\lambda}{l}\right)} = \frac{\sum_{k=1}^{\infty}\left\{\frac{1}{2k-1}\sin\left[\frac{(2k-1)\pi\lambda}{l}\right] - \frac{1}{2k}\sin\left[\frac{(2k)\pi\lambda}{l}\right]\right\}}{\sum_{n=1}^{\infty}\frac{1}{n}\sin\left(\frac{n\pi\lambda}{l}\right)}$$

or

$$\frac{P}{1-P} = -\frac{\pi\lambda}{l}\frac{\sum_{k=1}^{\infty}\left\{\frac{1}{(2k)\pi\lambda}\sin\left[\frac{(2k)\pi\lambda}{l}\right] - \frac{1}{(2k-1)\pi\lambda}\sin\left[\frac{(2k-1)\pi\lambda}{l}\right]\right\}}{\sum_{n=1}^{\infty}\frac{1}{n\pi\lambda}\sin\left(\frac{n\pi\lambda}{l}\right)\frac{\pi\lambda}{l}}.$$

Given that $\lambda \ll l$, the ratio of sums on the right-hand side can be considered as a ratio of two continuous integrals over the variables $(2k)\pi\lambda/l$ (numerator) and $n\pi\lambda/l$ (denominator),

$$\frac{P}{1-P} = -\frac{\pi\lambda}{l}\frac{\frac{1}{2}\int_0^{\infty}\frac{d}{dx}\left(\frac{\sin x}{x}\right)dx}{\int_0^{\infty}\frac{\sin x}{x}dx} = -\frac{\pi}{2}\frac{\lambda}{l}\frac{\left.\frac{\sin x}{x}\right|_0^{\infty}}{\int_0^{\infty}\frac{\sin x}{x}dx} = -\frac{\pi}{2}\frac{\lambda}{l}\frac{(-1)}{\frac{\pi}{2}}$$

or, eventually,

$$\frac{P}{1-P} = \frac{\lambda}{l}. \tag{18}$$

Substituting, now, λ in terms of the self-diffusivity from Eq. (12) into Eq. (18), we obtain

$$\frac{P}{1-P} = \frac{2D_s}{l\langle|v_x|\rangle} \quad \text{or } D_s = \frac{1}{2}l\langle|v_x|\rangle\frac{P}{1-P}. \tag{19}$$

If the mean speed along the x direction $\langle|v_x|\rangle$ is identified with l/τ, Eq. (19) is identical with Eq. (9). This identification is elaborated in the Appendix.

We have shown that a top down consideration of first passage through the slab boundaries, based on solving a continuous diffusion equation in the slab, leads to an expression equivalent to Eq. (9), which we derived from our mesoscopic second-order Markov process in a "bottom up" fashion, i.e., starting from molecular considerations. The location of the delta function in the initial condition of the continuous approach corresponds to the first step of a particle traveling at the thermal speed according to the displacement rules of the basic random walk.[4] This finding clarifies our assumption that λ should be a mean distance for velocity randomization. In a basic random walk, in fact, a particle entering into the interval at $x=0$ and reaching the position λ will subsequently have probability of $1/2$ to move to the left and probability of $1/2$ to move to the right.

III. RESULTS

A. Kinetic Monte Carlo experiment

We have constructed a kinetic Monte Carlo simulation, according to the displacement rules of the stochastic model (Sec. II B), in order to verify Eq. (9). The simulation worked as follows. We placed a particle at the origin of (one-dimensional) space, with a given orientation of its motion. We shot randomly to choose the kind of move to perform: with probability $1-P$, we left the particle in its actual position and reversed the direction of its motion; with probability P, we displaced the particle by a length l along the direction of its motion. At every step, we increased the simulation time by an interval τ. For each particle, we executed 10^2 steps, repeating the procedure for 10^7 different particles to compute the coefficient of self-diffusivity D_s by the traditional mean square displacement (MSD) procedure.[5] The whole experiment was repeated for various values of P in order to obtain a plot of the dimensionless quantity $D_s\tau/l^2$ as a function of P (see Fig. 3); it is seen that the simulation results are in perfect agreement with the theoretical formula.

B. Molecular dynamics experiments

To test our model, we performed equilibrium molecular dynamics simulations in the microcanonical (NVE) ensemble on a bulk system of soft spheres. For the particle-particle interaction, we used the repulsive part of the Lennard-Jones potential, truncated and shifted at the minimum (Weeks-Chandler-Andersen potential),[6,7]

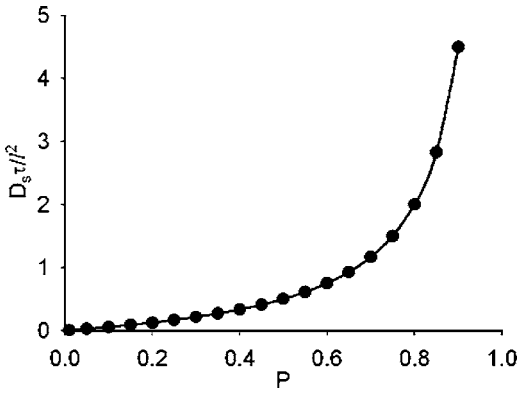

FIG. 3. Kinetic Monte Carlo results (circles) and plot of theoretical Eq. (9) (line) for the quantity $D_s\tau/l^2$ as a function of the transmission probability P.

$$U(r_{ij}) = \begin{cases} 4\varepsilon(\sigma^{12}/r_{ij}^{12} - \sigma^6/r_{ij}^6) + \varepsilon, & r_{ij} \leqslant 2^{1/6}\sigma \\ 0, & r_{ij} > 2^{1/6}\sigma. \end{cases} \tag{20}$$

In the following, all property values are reported in the corresponding Lennard-Jones units. The runs were performed with a time step $\delta t = 10^{-3}(m\sigma^2/\varepsilon)^{1/2}$, for a total of $2\times10^6 - 5\times10^6$ steps. Each run was repeated three times, in order to increase the accuracy of the measurements and compute the statistical error; statistical errors are omitted from the plots of results shown below, since they are always smaller than the symbol size.

Here, we describe the procedure for computing the equilibrium parameters relevant to our model (Sec. II B), namely, P and τ. To obtain the value of the transmission probability P, we use the relation

$$P = \lim_{t\to\infty} \frac{dn_T}{dn_S}, \tag{21}$$

where n_T is the number of transmission events and n_S is the number of state transitions (transmissions plus reflections) that take place in the whole simulation box. Remembering that a state transition implies that a particle has entered and subsequently exited a given slab, as a working procedure we will compute the number of state transitions by the number of slab exiting events that occur.

Looking at Eq. (3), the mean residence time spent by a particle in a slab, for a large number of state transitions (many slab exiting events) k, with a residence time τ_j inside each slab ($j=1,2,\ldots,k$), is calculable by the equation

$$\tau \equiv \langle\tau\rangle = \frac{t}{k}, \tag{22}$$

where $t=\Sigma_{j=1}^{k}\tau_j$.

Since we are interested in computing equilibrium averages, which imply long time scales, we can assume that each particle will sample all the possible velocities during its chain of state transitions. This fact, in parallel with the conservation of particle number N, allows distributing the average frequency of state transitions (frequency of slab exiting events), observed in the whole simulation box, among all the N particles, giving

$$\frac{1}{\tau} = \lim_{t\to\infty} \frac{1}{N}\frac{dn_S}{dt}. \tag{23}$$

The benefit of using Eq. (23), rather than computing directly the individual particle residence times, is that knowledge of only the global number of slab exiting events per unit time is needed. In fact, when we deal with high densities or very infrequent slab exiting events, it may happen that a specific particle performs, during the finite time of the simulation, no state transition at all, making Eq. (22) inapplicable (see Appendix for more details).

For the runs, the simulation box was set to a cubic unit cell of dimensions $10\sigma\times10\sigma\times10\sigma$, applying periodic boundary conditions along the three coordinate directions. The temperature was kept constant for all the runs, equilibrating the systems at $T=\varepsilon/k_B$. We sampled different values of the diffusivity, varying the density of the systems by changing the loadings of the unit cell from 100 to 1000 spheres.

To compute averages, during the run, we accumulated the desired quantity at every step and wrote it in a file every 10^4 time steps. This procedure allows monitoring eventual time drifts of the observed quantities; it is essential to the correct measurement of P and of the observables coming from the MSD routine; in fact, these averages reach an equilibrium value only after a characteristic time.

In particular, for the parameters τ and P, the slab width was chosen to be exactly one side of the unit cell, so that $l=10\sigma$. Then, whenever a particle exited the simulation box from either one of the two faces normal to the x axis and boundary conditions were applied, this was counted as a state transition. By accumulating in one variable the number of state transitions (slab exiting events) n_S through Eq. (23), we obtained the value of the mean residence time τ. To compute P, we also needed to accumulate the number of transmission events, namely, the occurrences of a particle exiting from the simulation box through a certain boundary along the x direction, provided that the previous exit, performed by the same particle, had taken place along the same direction of motion.

In Fig. 4, we can see an indicative procedure for computing $1/\tau$ and P for the system with $N=700$ particles. In this specific case, for the computation of the transmission probability, we started the data analysis after 4×10^4 events.

In Fig. 5, we display the values of the self-diffusivity, measured during the molecular dynamics (MD) runs via the usual mean square displacement procedure. In the same graph, we also present the values obtained by direct substitution of the average residence time and the forward probability, computed from the MD run, as described above, in the theoretical expression of Eq. (9).

At low densities there is a deviation between the diffusivity from the mean squared displacement and the one from Eq. (9). This is because the slab width is not large in comparison with the distance for particle velocity randomization, introducing correlations of higher order in the crossing of neighboring slabs (see Sec. IV B). The number of collisions and, hence, the degree of randomization increase with increasing loading.

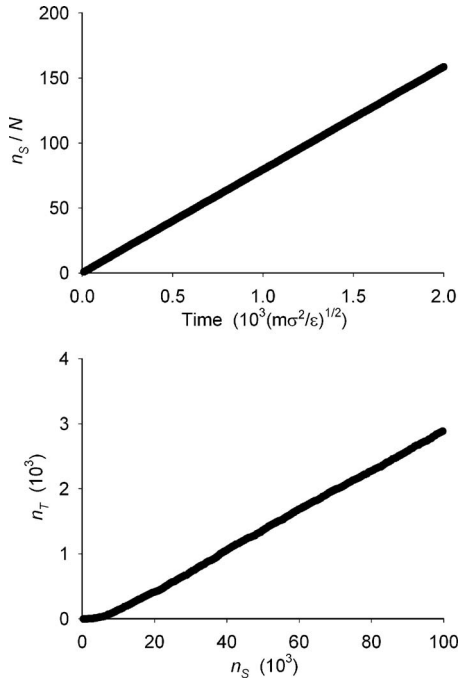

FIG. 4. Procedure followed for the calculation of the inverse of mean residence time (top) and the transmission probability (bottom).

In Fig. 6, we plot the mean residence time and the transmission probability as a function of number density. In a bulk system, the residence time τ is constant for given temperature and slab width (see Appendix); the deviations from a flat line are due to small differences in the average temperature of each system. On the other hand, P carries all the dependence on density (see Fig. 6). Note that, if one moves to a microporous system which is locally inhomogeneous, both the residence time and the forward probability are expected to be density dependent.

In Fig. 7, the velocity autocorrelation functions along the x direction are presented for $N=100$, 400, 700, and 1000 spheres per unit cell. It can be seen that a wide range of densities has been sampled, reaching nonmonotonic decay of the velocity autocorrelation function even with our purely repulsive particle-particle interaction.

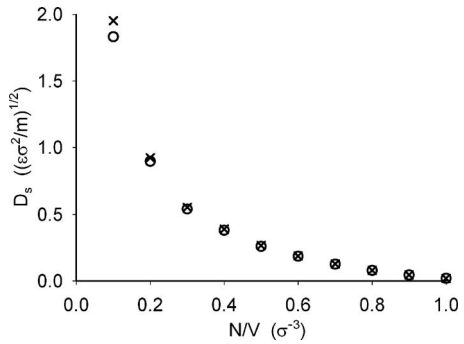

FIG. 5. Results from our mesoscopic model [Eq. (9)] (open circles) and from mean square displacement (crosses) for the self-diffusivity as a function of number density.

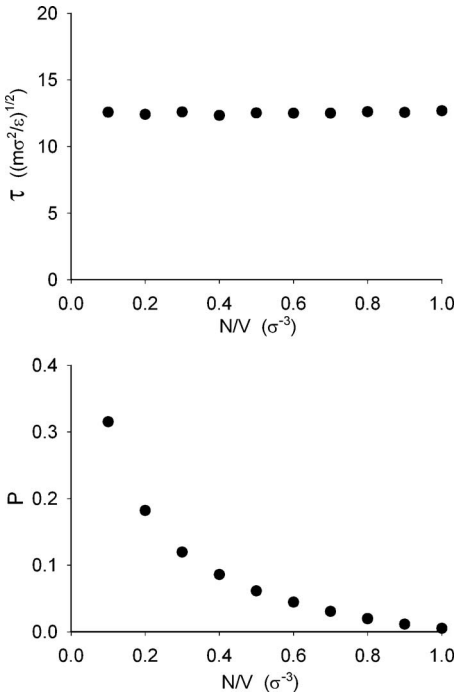

FIG. 6. Number density dependences of the mean residence time (top) and transmission probability (bottom).

IV. DISCUSSION

A. Dependence of the transmission probability *P* on the slab width *l*

In this section, we study the dependence of P on the width l of slabs. For this reason, we loaded our $10\sigma \times 10\sigma \times 10\sigma$ unit cell with $N=200$ particles and performed MD runs, as in the previous section. During the same run, we stored the number of transmission events n_T and state transitions n_S using slabs of 13 different widths; this allowed the simultaneous estimation of P for 13 different values of l. For these runs, we fixed the temperature at $T=2\varepsilon/k_B$ to increase the number of state transitions (slab exiting events), so that better statistics is attained. In Table I, we can see the computed values of P for various widths.

During the MD run, the computed coefficient of self-diffusion, via the usual MSD procedure, was $D_s = (1.394 \pm 0.011)(\varepsilon\sigma^2/m)^{1/2}$. In Fig. 8, this value is compared with the ones obtained by substituting in Eq. (9) the values of P for the various values of l (Table I). The value of $l/\tau = (1.123 \pm 0.001)(\varepsilon/m)^{1/2}$ has also been computed during the MD run. It is constant for all the slab widths, i.e., $1/\tau$ is

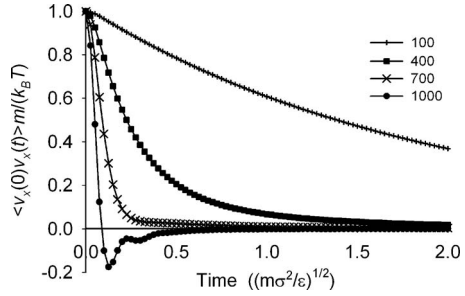

FIG. 7. Velocity autocorrelation functions for various loadings.

TABLE I. Influence of slab width l on the transmission probability P.

$l(\sigma)$	P
0.10	0.9397
0.25	0.8720
0.50	0.7872
1.00	0.6685
2.50	0.4712
10.00	0.1943

inversely proportional to l, since the width of the slabs determines the number of slabs in which the system is divided (see Appendix).

We can clearly see that our model becomes more accurate upon increasing the slab width. In Fig. 8, it is seen that, as l increases, the value of self-diffusivity, computed through the theoretical expression of our model [Eq. (9)], converges asymptotically to the one computed by MSD D_S^{MSD}; then, we can write

$$\lim_{l\to\infty}\left(\frac{lP}{1-P}\right) = \frac{2\tau D_s^{\mathrm{MSD}}}{l} = \mathrm{const} \quad \text{or} \lim_{l\to\infty}\frac{1-P}{P} = \frac{1}{\mathrm{const}}l,$$

which is also suggested by Eq. (18). Therefore, the plot of quantity $(1-P)/P$ should become linear as l grows, exhibiting a constant slope. This is confirmed in Fig. 9.

We see that for small l the curve is not linear. This means that, for small values of l, the consecutive moves of the spheres have a degree of correlation, not allowing the correct evaluation of P. To compute more precisely the self-diffusion coefficient, then we need to refine our procedure and evaluate the slope of the $(1-P)/P$ curve as l goes to infinity; we define this quantity as

$$\frac{1}{\zeta} = \lim_{l\to\infty}\frac{d\left[\frac{1-P}{P}\right]}{dl} = \lim_{l\to\infty}\frac{d(1/P)}{dl}. \tag{24}$$

Thus, a more complete expression for the self-diffusivity is provided by

$$D_s = \frac{1}{2}\frac{l}{\tau}\zeta. \tag{25}$$

Interpolating the curve of Fig. 9, we obtain $1/\zeta = (0.410 \pm 0.005)\sigma^{-1}$. Our best estimation of the self-diffusion

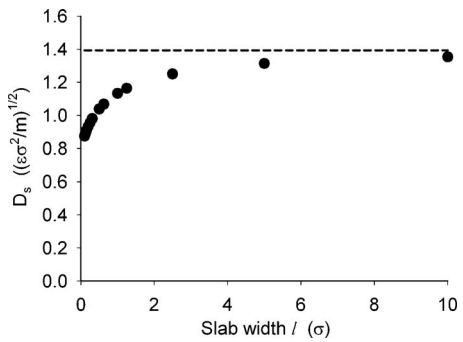

FIG. 8. Self-diffusivity estimated via Eq. (9) for various values of slab width l (circles), the dashed line indicates the computed D_s from molecular dynamics through MSD.

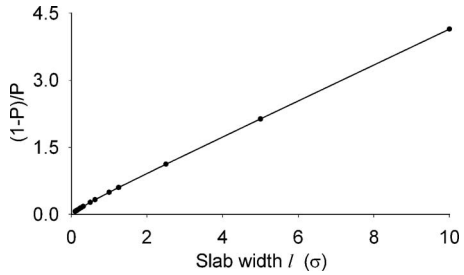

FIG. 9. Plot of $(1-P)/P$ as a function of slab width; the line is a guide for the eyes and shows the departure from linearity at small values of l.

coefficient is then $D_s=(1.37\pm0.02)(\varepsilon\sigma^2/m)^{1/2}$, in perfect agreement with the value computed through the mean square displacement routine.

B. Microscopic aspects of self-diffusivity

The nonlinearity at small slab widths of the curve in Fig. 9 shows that, on the considered space scale, there is a correlation between the consecutive moves of each single particle. For low densities, it happens that a particle crosses a given slab with a transmission event and then retains enough velocity to cross also the next slab with a transmission event, without suffering an effective randomization of its velocity. In our model, the randomization is ensured when the particle inverts the direction of its motion at least once in each slab. The correlation of the moves means that after a transmission event, there is a probability, higher than P, that the same particle will suffer another transmission event. Under these conditions, using directly Eq. (9), we have an underestimation of the diffusivity.

Instead, for very high densities, it may happen that, after a transmission event, there is a probability lower than P that the same particle will suffer another transmission event. This occurs when a particle, caged in by its neighbors, spends some time oscillating about a mean position before suffering an effective displacement. Under these conditions, direct application of Eq. (9) would overestimate the self-diffusivity.

Our stochastic model coarse grains the microscopic nature of self-diffusivity, which is shaped by the distances traveled by the particles between two consecutive inversions of their direction of motion (inversion paths). These inversions are clearly generated by the collective effect of collisions with other particles; the number of collisions needed to provoke an inversion depends on the system parameters.

Figure 10 shows a plot of the inversion path distribution computed for the loadings $N=100$ and 1000 at $T=\varepsilon/k_B$. For low densities, the tail of the distribution is very long (region A) and this leads to the underestimation of P if the slab width is too small; while for high densities, due to the cage-in effect, the initial part of the distribution presents a pulselike shape (region B) which accounts for the overestimation of P when slabs smaller than the pulse width are used.

C. Approach to linearity

In this section, we want to study how the curve $(1-P)/P$ attains linearity as the width of the slabs l is increased, for different conditions of temperature, density, and particle-particle interaction. We use the previously mentioned procedure to compute P for different slab widths, applying it to loadings $N=100$, 400, 700, and 1000 at $T=\varepsilon/k_B$ and loadings $N=200$, 400, 600, and 800 at $T=2\varepsilon/k_B$. Then, we also change the shape of the potential, using

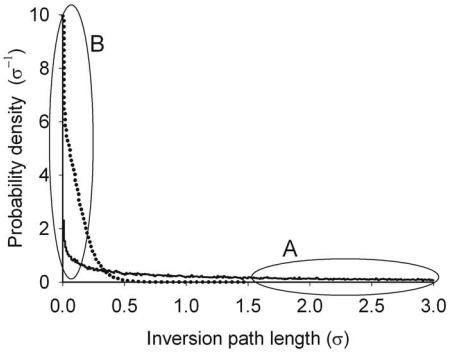

FIG. 10. Distribution of inversion paths for $N/V=0.1\sigma^{-3}$ (line) and $N/V=1\sigma^{-3}$ (dots). Region A shows the long tail of the distribution at low density, while region B shows the pulselike shape for the distribution at high density.

$$U(r_{ij})=\begin{cases}4\varepsilon(\sigma^8/r_{ij}^8-\sigma^4/r_{ij}^4)+\varepsilon, & r_{ij}\leqslant 2^{1/4}\sigma\\ 0, & r_{ij}>2^{1/4}\sigma\end{cases}$$

to perform runs for $N=200$, 400, and 600 at $T=2\varepsilon/k_B$. With the latter potential, the diameter of the spheres is bigger than those in the previous systems, and their repulsion is softer.

In Fig. 11, we plot $(1-P)/P$ for all the different systems. Applying a linear regression procedure to the curves of Fig. 11, we see that the intercept of the interpolating lines would not pass through the origin, explaining why we need to evaluate $1/\zeta$ and use Eq. (25) to get a correct value of D_s, rather than using the theoretical second-order Markov process [Eq. (9)].

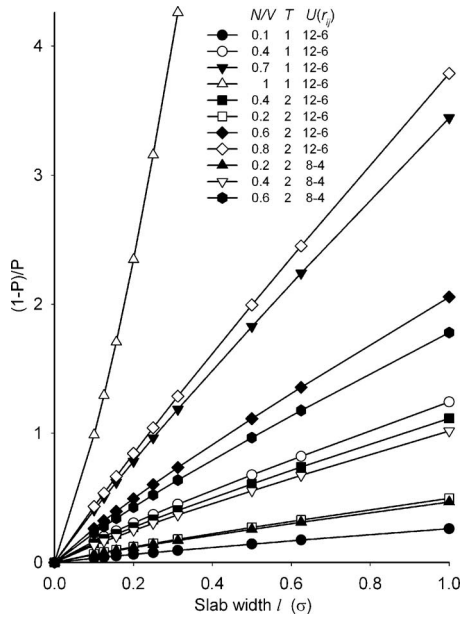

FIG. 11. Plots of $(1-P)/P$ for the various systems simulated at different densities $N/V(\sigma^{-3})$, temperatures $T(\varepsilon/k_B)$, and shapes of the potential $U(r_{ij})$.

It is interesting to note that the different $(1-P)/P$ curves do not cross each other, at least for the cases investigated here. For this reason, each pair of values $(l,(1-P)/P)$, defining a point in the plane of Fig. 11, corresponds to one and only one value of $1/\zeta$.

In other words, the approach to linearity of the different curves, namely, the way they attain their limiting slope $1/\zeta$, depends only on the value of $1/\zeta$ itself and not on density, temperature, or particle interaction. This is not the case for the MSD procedure, where there is no unique correspondence between the region of nonlinear response and the limiting slope of the linear region.

To have a good evaluation of $1/\zeta$, the best approach is to measure the transmission probability for at least two different widths l, using wide enough slabs to avoid correlation in the moves. *A posteriori*, after that $1/\zeta$ is obtained, it is possible to evaluate the goodness of the computation, estimating via Fig. 11 the minimum width l required to be in the linear part of the $(1-P)/P$ curve, for the computed value of $1/\zeta$.

V. CONCLUSIONS

We have developed a technique to coarse grain the translational motion of molecules in a system at equilibrium, modeling it through a second-order Markov chain. We have also shown how the self-diffusion coefficient can be computed through this model.

The coarse graining is performed by averaging the dynamics over regions of space (slabs) of fixed dimension l, dealing with only one principal direction at a time. Important parameters of the model are the transmission probability P and the mean residence time τ. From those, one can estimate the characteristic step length ζ and the characteristic velocity l/τ which determine the diffusivity. In a bulk system, P or ζ incorporates practically all the density dependence of the diffusivity, with l/τ being a temperature-dependent but density-independent thermal speed.

We have tested the model extensively against molecular dynamics simulations over a wide range of densities, confirming and clarifying its predictions. We have also shown that the expression given by the model for the self-diffusivity is consistent with a top down analysis of first passages based on a continuum diffusion equation.

ACKNOWLEDGMENTS

Support by the European Union via the FP6-Marie Curie Research Training Network "INDENS" (No. MRTN-CT-2004-005503) is gratefully acknowledged. M.S. is grateful to Dr. Jean-Marc Leyssale, postdoctoral fellow of the above program, for his training on computing and to Dr. Adrien Leygue for the helpful discussions.

APPENDIX: DEPENDENCE OF MEAN RESIDENCE TIME ON SLAB WIDTH

We take a closer look at the formula of the average frequency of slab exit events [Eq. (23)]. For identical slabs, disposed perpendicularly to the x direction, we can generalize $\lim_{t\to\infty}(dn_s/dt)=(L/l)\langle|v_x|\rangle\rho(x_0)$, where L is the length of the simulation box along the x direction, L/l is the number of slabs, and $\rho(x_0)=\int_A c(x_0,y,z)dydz$ is the linear density, averaged over the boundary surface A, located at x_0. The normalization condition for the density function is $N=\int_V c(x,y,z)dxdydz$. Then, we can rewrite Eq. (23) as $1/\tau=(L/N)[\langle|v_x|\rangle\rho(x_0)/l]$. We note that $1/\tau$ is an intensive quantity, being independent of the size of the system, since the width of the slab l is arbitrarily fixed. The term N/L is the mean linear density of particles along the x direction, while $\rho(x_0)$ is the corresponding local property, depending on the boundary location. We can define the parameter $\alpha=(L/N)\rho(x_0)$, which gives the model velocity $l/\tau=\langle|v_x|\rangle\alpha$ that particles have in the coarse-grained picture of our second-order Markov process. In the bulk case, excluding phenomena of ordering transition, the density $\rho(x,y,z)$ is homogeneous so that $\rho(x_0)=N/L$ and $\alpha=1$. Thus, we can write

$$\frac{1}{\tau}=\frac{\langle|v_x|\rangle}{l}, \tag{A1}$$

which ensures that the mean residence time is linearly proportional to the slab width l.

During the MD runs of Sec. III B, made with loadings from 100 to 1000 molecules in a box of edge length 10σ and a purely repulsive modification of the (12-6) Lennard-Jones

TABLE II. MD computation of average temperature T and mean residence time τ for various densities N/V. Evaluation of mean residence time from the Maxwell-Boltzmann relation $\tau_{\text{theor}}=\sqrt{\pi ml^2/2k_BT}$ and comparison with the MD result $|\text{delta}|=(|\tau_{\text{theor}}-\tau|/\tau_{\text{theor}})\cdot 100$. The slab width is $l=10\sigma$, while τ_{theor} is in the same units as τ.

N/V (σ^{-3})	T (ε/k_B)	τ $(m\sigma^2/\varepsilon)^{1/2}$	$\sqrt{\pi ml^2/2k_BT}$	|Delta| (%)
0.1	0.996	12.572	12.555	0.14
0.2	1.018	12.411	12.420	0.07
0.3	0.995	12.585	12.563	0.17
0.4	1.041	12.328	12.281	0.38
0.5	0.997	12.522	12.552	0.24
0.6	1.006	12.501	12.494	0.05
0.7	1.004	12.508	12.507	0.01
0.8	0.989	12.608	12.598	0.08
0.9	0.999	12.552	12.539	0.11
1.0	0.979	12.684	12.662	0.17

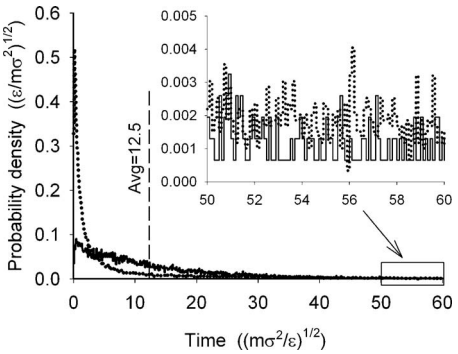

FIG. 12. Distribution of residence times for $N/V=0.1\sigma^{-3}$ (line) and $N/V=0.4\sigma^{-3}$ (dots), the dashed line shows the mean residence time for both distributions $\tau=12.5(m\sigma^2/\varepsilon)^{1/2}$. The inset is a zoom for the long time region to show that the distribution of the denser system has a longer tail.

interaction, we have computed the average temperature T of the system (which was set to be near ε/k_B) and the mean residence time. From the Maxwell-Boltzmann distribution of velocities, we know that $\langle|v_x|\rangle=\sqrt{2k_BT/\pi m}$; through substitution in Eq. (A1), we obtain

$$\frac{1}{\tau}=\sqrt{\frac{2k_BT}{\pi ml^2}}.$$

In Table II, we compare the mean residence time obtained through the Maxwell-Boltzmann relation with the value computed directly during the MD run; the percentile discrepancy between the two values is always lower than 0.4%, showing good agreement.

With the same system, we have also evaluated the distribution of the mean residence time for the loadings $N=100$ and 400 at $T=\varepsilon/k_B$. Here, we have measured the difference between the time of exit and the time of entry of every particle in each slab visited (compare Sec. III B) and plotted the distribution of this difference in Fig. 12.

The mean value is the same for both distributions, even though the shape of the distribution is different. As the density increases, we have many particles that spend a short time inside the slab but also many others that spend a very long time inside the slab; in other words, the distribution becomes broader. As previously mentioned, at equilibrium, we know that each particle will sample, in a long enough time, all the accessible velocity states, making the shape of the distribution of residence times irrelevant for what concerns the coefficient of self-diffusion.

[1] A. Einstein, Ann. Phys. **17**, 549 (1905).
[2] P. W. Atkins, *Physical Chemistry*, 4th ed. (Freeman, New York, 1990).
[3] J. Crank, *The Mathematics of Diffusion*, 2nd ed. (Clarendon, Oxford, 1975).
[4] F. Reif, *Fundamentals of Statistical and Thermal Physics* (McGraw-Hill, New York, 1965).
[5] M. P. Allen and D. J. Tildesley, *Computer Simulation of Liquids* (Clarendon, Oxford, 1989).
[6] J. D. Weeks, D. Chandler, and H. C. Andersen, J. Chem. Phys. **54**, 5237 (1971).
[7] D. Frenkel and B. Smit, *Understanding Molecular Simulation*, 2nd ed. (Academic, San Diego, 2002).